J Sol-Gel Sci Technol (2015) 73:655–659
DOI 10.1007/s10971-015-3615-6

ORIGINAL PAPER

Hydrothermal growth of bilayered rutile-phased TiO_2 nanorods/ micro-size TiO_2 flower in highly acidic solution for dye-sensitized solar cell

M. K. Ahmad · V. M. Mohan · K. Murakami

Received: 21 June 2014 / Accepted: 2 January 2015 / Published online: 20 January 2015

Abstract Aligned rutile-phased TiO_2 (r-TNRs) nanorods and micro-size rutile-phased TiO_2 flowers (r-TFs) films were prepared on fluorine-doped tin oxide (FTO) substrate using highly acidic solution by two steps of hydrothermal process. The hydrothermal process was done at 150 °C in 5 h for the first step and 2 h for the second step. These films were used as a photoelectrode in dye-sensitized solar cell (DSC) application. Aligned r-TNRs and r-TFs were prepared using one-step and two-step hydrothermal processes, respectively. At the end of second step hydrothermal process, micro-size rutile-phased TiO_2 flowers (r-TFs) were observed on top of r-TNRs (FTO/r-TNRs/r-TFs). Power conversion efficiencies for both aligned r-TNRs and r-TNRs/r-TFs were compared. From the results, DSC made of r-TNRs only produced energy conversion efficiency of 1.52 % and DSC made of r-TNRs/r-TFs gave excellent energy conversion efficiency (η) of 4.27 %.

Keywords Titanium dioxide · Nanorods · TiO_2 flower · Rutile · Power conversion efficiency · Hydrothermal

1 Introduction

Since 1991 when the DSC was first reported by Grätzel's group, it has been widely studied due to the low cost of manufacturing and simple preparation process [1, 2]. There were many researchers who intended to produce various types of DSCs [3] including the rutile-phased TiO_2-based DSC [4, 5]. However, there was no report in rutile-based DSC which has a bilayered structure such as the rutile-phased TiO_2 flowers (r-TFs) layer on top of the aligned r-TNRs layer.

Conventionally, one-dimensional (1D) TiO_2-aligned nanostructure such as nanorods can be prepared using anodization electrochemical of titanium [6, 7], template-assistant approaches [8, 9], direct oxidation of Ti substrate [10], metal–organic chemical vapor deposition [11, 12] and hydrothermal synthesis [13, 14]. Among these methods, hydrothermal synthesis is a simple method because of its easy preparation and cost effective. Therefore, hydrothermal process is a promising approach to prepare well-aligned TiO_2 nanostructures in large scale. Although 1D TiO_2-aligned nanostructures material has been extensively studied, the preparation of TiO_2 nanorods and flower-like TiO_2 structures on substrates via hydrothermal method was rarely reported.

Feng et al. [15] fabricated TiO_2 nanorod films grown on glass substrates using a low-temperature hydrothermal method. Kakiuchi et al. [16] reported the preparation of rutile TiO_2 rods on glass substrates at low temperature of unmodified glass substrates through heterogeneous nucleation in hydrothermal solution. However, because the used substrates were amorphous, TiO_2 crystal nucleus from the precursor solution formed irregularly on the substrates. Therefore, aligned TiO_2 nanorods have grown randomly with poor orientation. Liu et al. [17] have synthesized oriented, single-crystalline rutile-phased TiO_2 nanorods on unmodified fluorine-doped tin oxide conductive glass (FTO) substrates using titanium butoxide as precursor by hydrothermal method. However, it was difficult to achieve

M. K. Ahmad (✉)
Microelectronics and Nanotechnology-Shamsuddin Research Centre (MiNT-SRC), Universiti Tun Hussein Onn Malaysia, 86400 Batu Pahat, Johor, Malaysia
e-mail: akhairul@uthm.edu.my

V. M. Mohan · K. Murakami
Research Institute of Electronics, Shizuoka University, Hamamatsu, Shizuoka 432-8011, Japan

controllable growth of TiO_2 nanorods, and it has been proven that this method cannot be used on other substrates in order to grow oriented TiO_2 nanorods. In our previous works, both aligned TiO_2 nanorods and flower-like TiO2 structure were grown on FTO substrate at the same time using hydrothermal method [18, 19].

We investigated the advantages of bilayer structure which were prepared by highly acidic solution in hydrothermal method at low temperature. The novelty of the study is the combination of both r-TNRs and r-TFs in the construction of rutile-based DSC. We previously reported our success in producing these two types of nanostructures with a power conversion efficiency of 3.11 % [19]. In this study, we would like to report a two-step production of r-TNRs and r-TFs, whereby a r-TNRs layer is initially produced followed by a layer of r-TFs on top of it. We have optimized the parameter involved. By combining the two types of TiO_2 nanostructure in a rutile-based DSC, the amount of dye absorbed onto the surface of TiO_2 nanostructure was significantly improved, improving the performance of rutile-based DSC.

2 Experimental

Fluorine-doped SnO_2 (FTO) with a thickness of 1.0 μm coated on glass was used as a substrate. Ethanol, acetone, hydrochloric acid (HCl) and titanium butoxide (TBOT) (WAKO chemical) were used for the preparation of solution using deionized (DI) water. The FTO-coated glass was cut into the desired dimension of 10 mm × 25 mm and cleaned by sonicating method in acetone, ethanol and DI water with the volume ratios of 1:1:1 for 30 min followed by drying in the air. Synthesis of the film on the FTO substrate was performed according to the previous study with some improvement [6]. For the r-TNRs layer, the chemical solution for hydrothermal process was prepared by dissolving 120 ml of concentrated HCl (36.5–38 %) in a 120 ml of DI water. The mixture was vigorously stirred for 5 min and then 6.0 ml of TBOT was added by drop wise using capillary tube. After stirring for 10 min, the solution was put into a steel-made autoclave with Teflon-made liner (300 ml) for hydrothermal process in which the FTO glass substrates were put with a conducting FTO surface facing upward. The hydrothermal process was performed at 150 °C for 5 h. After this first hydrothermal process, the autoclave was taken out from oven and cooled down to room temperature. The prepared samples were rinsed with DI water for 5 min and dried at room temperature.

For the r-TFs overlayer, the solution was prepared by mixing 80 ml of DI water and 8 ml of HCl. The solution was stirred for 5 min and then 2.84 g of cetyltrimethylammonium bromide (CTAB) was added as a surfactant. Finally, 1.5 ml of TBOT was added by drop wise into the solution. This solution was stirred for 10 min and then put into 300 ml Teflon-made autoclave together with substrates on which the r-TNRs layers were already prepared in the first step of hydrothermal process. The substrates were put into the autoclave with the r-TNRs side facing upward. The second hydrothermal process was done at 150 °C for 2 h. After the hydrothermal process, the samples were rinsed with DI water and annealed at 450 °C for 30 min. Finally, the DSCs were fabricated using the films as photoelectrode.

Surface morphology, cross section and thickness of the prepared TiO_2 films were observed by using field-emission scanning electron microscopy (FE-SEM, JEOL JSM-6320F) at accelerating voltage of 20 kV. X-ray diffraction (XRD, Rigaku RINT Ultima III) was performed with Cu Kα radiation ($\lambda = 1.5418$ Å). The XRD patterns were measured in the 2θ range from 20° to 50° with 2°/min scanning speed to investigate the crystal phases of TiO_2 films.

Photocurrent versus voltage (I–V) characteristics and incident photon to current efficiency were measured by using solar simulator (JASCO CEP-25 BX) under 1.5 AM. The prepared TiO_2 photoelectrode with an area of 0.25 cm^2 was immersed into 3 mM of N719 dye for about 14 h at room temperature. The Pt counter electrode with mirror finish was prepared by the sputtering method and used as counter electrode. In order to complete the assembly of the DSC, dimethyl-propyl-benzimidiazole iodide (DPMII) electrolyte was used and prepared from 0.6 M of 1,2-dimethyl-3-propylimidazolium iodide, 0.1 M of lithium iodide, 0.5 M of 4-tert-butylpyridine, 0.1 M of guanidine thiocyanate, 0.85 ml of acetonitrile, 0.5 ml of valeronitrile and 0.05 M of Iodine. The electrolyte was inserted between the Pt electrode and the dye-coated r-TNRs/r-TFs electrode to form a sandwich-type clamped cell.

3 Results and discussion

XRD patterns of the r-TNRs layer and r-TNRs/r-TFs bilayer are shown in Fig. 1. The result shows three peaks detected at 27.40°, 36.04° and 43.90° corresponding to (110), (101) and (110) planes of the rutile phase (PDF No. 98-000-0090). The main peak was the (110) plane. Any additional peaks were not detected except the peaks originated from the FTO layer. There were slight increases in all peak intensities for the r-TNRs/r-TFs bilayer because the crystallinity of the layer was improved by the annealing treatment. It was confirmed from the result that the both prepared TiO_2 films were rutile.

The surface morphologies of r-TNRs layer and r-TNRs/r-TFs are shown in Fig. 2. Fig. 2a shows the high-magnification SEM image of layer surface, which reveals that the layer was composed of dense nanorods which were square

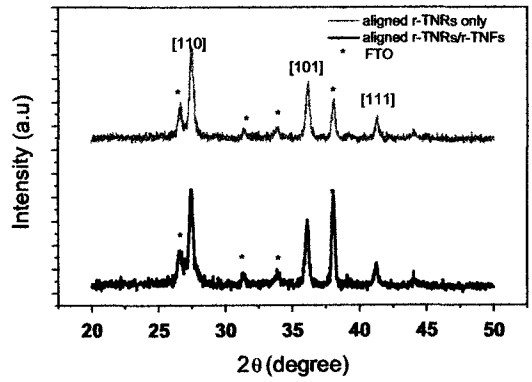

Fig. 1 XRD patterns of the r-TNRs layer and the r-TNRs/r-TFs bilayer

and diameters range between 50 and 300 nm. It was also observed that the nanorods were well vertically oriented and uniformly deposited on the FTO layer as shown in Fig. 2b. Thickness of the aligned r-TNRs layer is found to be 3 μm. Figure 2d confirms that the r-TFs layer was grown on the top of aligned r-TNRs layer through the two-step hydrothermal process. The size of each nanoflower was found to be about 1 μm in diameter, and each nanoflower was assembled by many nanorods joining with one end as shown in the magnified SEM image (Fig. 2c).

Surface morphology of the r-TNRs/r-TFs bilayer also revealed that the bilayer was very porous and composed of much amount of nanoflowers on the well-aligned nanorods, and that the total thickness of bilayer was 20 μm. The bilayer film structure was favorable for dye adsorption due to its very high surface area. It is also expected that the DSC fabricated using bilayer film as a photoelectrode can improve its photovoltaic performance.

Figure 3 shows incident photon to current conversion efficiency (IPCE) spectra of the DSCs fabricated using the aligned r-TNRs and aligned r-TNRs/r-TFs bilayer as a photoelectrode. The conversion of photons to electrons of the two photo anodes was observed in the wavelength range between 400 nm and 800 nm with a maximum conversion at 530 nm. The r-TNRs/r-TFs bilayered photoelectrode gave higher IPCE value over the whole spectral range mainly due to a larger amount of dye adsorption. IPCE is a measure of how efficiently our solar cell converts incident light into electrical energy at a given wavelength. In other words, IPCE measures how many electrons are excited when a light is illuminated to the solar cell. When light is illuminated to DSC, dye molecules will absorb the light and electrons in the dye molecules will be excited. When DSC with only nanorods was illuminated, the highest percentage of IPCE was 0.13 %. However, when DSC with bilayered photoelectrode was illuminated, the highest percentage of IPCE was 0.6 %. We can see that, there is an increment of about 0.47 %. This increment is due to improvement in the amount of excited electrons

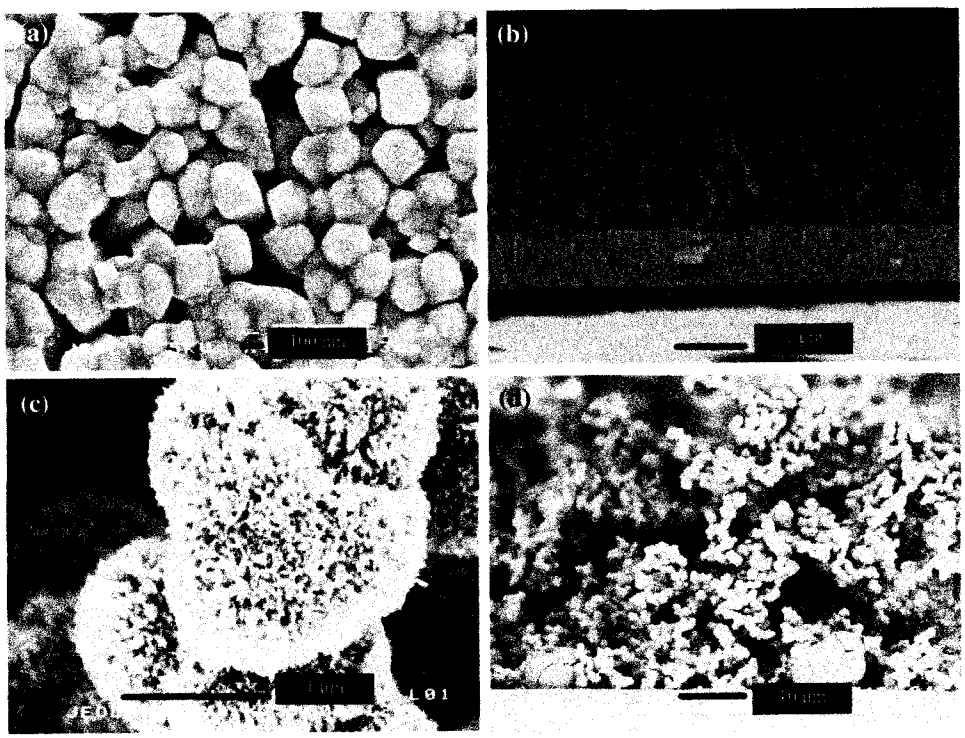

Fig. 2 SEM images of **a** the top view of aligned r-TNRs layer, **b** its cross section, **c** top view of the r-TNRs/r-TFs bilayer and **d** its cross section

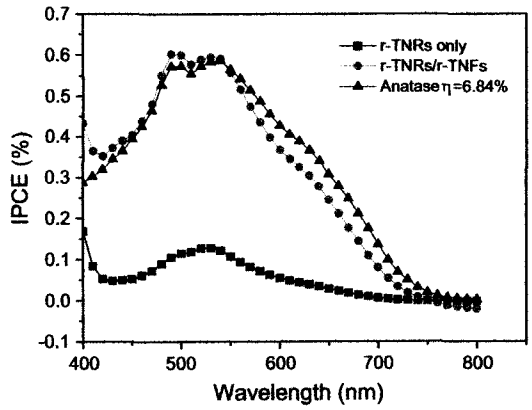

Fig. 3 IPCE spectra of the DSC fabricated using aligned r-TNRs layer, r-TNRs/r-TFs bilayer and anatase-phased TiO_2 as a photoelectrode

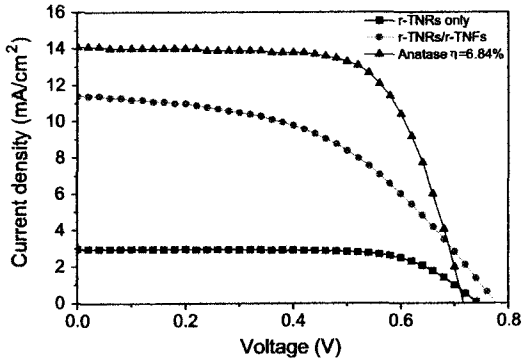

Fig. 4 Photocurrent–voltage characteristics of the DSC fabricated using aligned r-TNRs layer, r-TNRs/r-TFs bilayer and anatase-phased TiO_2 as a photoelectrode

when the DSC is illuminated with light. The large amount of excited electrons is contributed by the large amount of dye molecules absorbed onto the r-TFs of the DSC with bilayered photoelectrode.

In the IPCE spectrum of DSC based on the r-TNRs/r-TFs bilayer, some sort of hump can be seen in the wavelength between 600 and 650 nm as shown in Fig. 3. It cannot be seen in the spectrum for r-TNRs layer. This phenomenon might be explained by a light scattering effect which enhances the light harvesting in the layer. The nanoflowers can become light scatterers due to their size of 1 μm.

Photocurrent–voltage characteristics of the DSC fabricated using aligned r-TNRs layer and r-TNRs/r-TFs bilayer as a photoelectrode are shown in Fig. 4 under the simulated one sunlight with intensity of 100 mW cm^{-2}. The photovoltaic properties such as short-circuit current density (Jsc), open-circuit voltage (Voc), the fill factor (FF) and energy conversion efficiency (η) were summarized in Table 1. The Jsc for the r-TNRs/r-TFs bilayered photoelectrode increased drastically to 11.29 mA/cm^2 from 2.98 mA/cm^2 for the aligned r-TNRs single-layered photoelectrode. In the case of r-TNRs/r-TFs bilayered photoelectrode, the specific surface area and the porosity of film were increased by the existence of r-TFs layer as shown in Fig. 1, and the dye adsorption in the film was enhanced. Furthermore, the aligned r-TNRs layer under the r-TFs layer enhanced the transportation of photo-generated electrons from the r-TFs layer to the FTO substrate due to the higher electron mobility property. However, only small difference was seen in the amount of dye adsorption between the r-TNRs single layered and the r-TNRs/r-TFs bilayered photoelectrodes as shown in Table 1, while the difference in efficiency was very large due to improvement in current density (Jsc). It is suggested from this result that the dye molecules were adsorbed into r-TNRs layer both chemically and physically. Since the surface of layer was very flat, it became easy to adsorb more dye molecules on the chemisorbed dye molecules resulting in a significant amount of total adsorbed dye molecules.

The Voc was slightly higher for the r-TNRs/r-TFs bilayered photoelectrode, which can be explained by a charge recombination between the film and the dye or the electrolyte. In the case of r-TNRs single-layered photoelectrode, larger bare surface areas of nanorods are faced to the electrolyte even after the dye sensitization due to the density of nanorods as shown in Fig. 4b. It became difficult for the electrolyte to diffuse into r-TNRs layer through the thick r-TFs layer for the r-TNRs/r-TFs bilayer photoelectrode.

In order to study the advantages of r-TNRs/r-TFs bilayered photoelectrode for the DSC application, the photovoltaic properties were compared with the DSC fabricated using anatase-phased TiO_2 photoelectrode in our previous study [20]. The IPCE spectra, the I–V characteristics and the photovoltaic properties were also depicted in Figs. 3 and 4, and listed in Table 1, respectively. It is found from the result that more dye adsorption gave higher efficiency of the anatase-phased TiO_2 photoelectrode. There is, however, only small difference in the IPCE spectra, which did not correspond to the difference in dye adsorption and suggests a potential availability of the high efficiency DSC based on the rutile-phased TiO_2 film. As clarified in Table 1, the DSC fabricated using r-TNRs/r-TFs bilayered photoelectrode gave the lowest fill factor mainly originated from the poor electrical contacts between r-TFs layer and r-TNRs layer. If the contacts are improved and the fill factor becomes the value similar to other two DSCs, the efficiency is also improved to become around 6 %. This suggests that the DSCs fabricated using r-TNRs/r-TFs bilayered photoelectrode could realize higher performance DSC than the anatase-phased TiO_2-based DSC with the same amount of dye adsorption due to the higher

Table 1 Photovoltaic properties derived from Fig. 4 and those for the DSC based on anatase-phased TiO_2 photoelectrode

Sample	Voc	Jsc (mA cm^{-2})	Fill factor	Efficiency (%)	Dye adsorption (mol cm^{-2})
r-TNRs layer	0.74	2.98	0.68	1.52	5.55×10^{-8}
r-TNRs/r-TNFs bilayer	0.77	11.29	0.49	4.27	8.71×10^{-8}
Anatase-phased TiO_2	0.71	14.08	0.68	6.56	1.92×10^{-7}

electron mobility property of rutile-phased TiO_2. The light scattering effect was also seen in the IPCE spectra for the anatase-phased TiO_2 photoelectrode because the anatase-phased TiO_2 film was prepared from two kinds of TiO_2 particle sizes and composed of fine grains and agglomerated grains. As in our previous results, it gave the same idea for enhancing the performance of rutile-based DSC [6]. The result suggests that better dye adsorption will improve the performance of rutile-based DSC.

4 Conclusion

In this study, we prepared aligned r-TNRs directly on top of FTO substrate and the r-TFs grown on the top of aligned r-TNRs by two-step hydrothermal process. The dye adsorption and light harvesting effect increased due to the top layer r-TFs and obtaining the good electron mobility due to the aligned nanorods as base layer. We achieved short-circuit current intensity of 11.29 mA cm^{-2} and light to electricity conversion efficiency of 4.27 % by using very densed 3-μm-long aligned r-TNRs/r-TFs as the photo anodes in DSC. The performance of rutile-based DSC was improved due to the better dye adsorption and light harvesting effect from the r-TFs film.

The DSCs fabricated using r-TNRs/r-TFs bilayered photoelectrode could realize the higher performance DSC than the anatase-phased TiO_2-based DSC with better electrical contacts between r-TFs layer and r-TNRs layer. The DSC fabricated using these r-TNRs-/r-TFs-based photoelectrode gave excellent energy conversion efficiency (η) of 4.27 %.

Acknowledgments The authors would like to thank to Ministry of Education (MOE), Malaysia, Research Institute of Electronics, Shizuoka University and Universiti Tun Hussein Onn Malaysia (UTHM) for Exploratory Research Grant Scheme (ERGS) Vot E022.

References

1. Regan B, Gratzel M (1991) Nature 353:737–740
2. Gratzel M (2003) J Photochem Photobiol C 4:145–153
3. Hao P, Jieshu Q, Ang Y, Meigui X, Luo T, Qingli C, Xingfu Z (2011) Appl Surf Sci 257:5059–5063
4. Hong Z, Jie T, Tao W, Jie D (2011) Appl Surf Sci 257: 10494–10498
5. Francis L, Nair SA, Jose R, Ramakrishna S, Thavasi V, Marsano E (2011) Energy 36:627–632
6. Paulose M, Shankar K, Yoriya S, Prakasam HE, Varghese OK, Mor GK, Latempa TA, Fitzgerald A, Grimes CA (2006) J Phys Chem B 110:16179–16184
7. Yang Y, Wang XH, Li LT (2008) Mater Sci Eng B 149:58–62
8. Huang CM, Liu XQ, Liu YP, Wang YY (2006) Chem Phys Lett 432:468–472
9. Attar AS, Ghamsari MS, Hajiesmaeibaigi F, Mirdamadi S, Katagiri K, Koumoto K (2009) Mater Chem Phys 113:856–860
10. Peng X, Chen A (2005) Appl Phys A 80:473–476
11. Pradhan SK, Reucroft PJ, Yang F, Dozier A (2003) J Cryst Growth 256:83–88
12. Maekawa T, Kurosaki K, Tanaka T, Yamanaka S (2008) Surf Coat Technol 202:3067–3071
13. Yun H, Lin CJ, Li J, Wang JR, Chen HB (2008) Appl Surf Sci 255:2113–2117
14. Li G, Liu ZQ, Zhang Z, Yan X (2009) Chin J Catal 30:37–42
15. Feng XJ, Zhai J, Jiang L (2005) Angew Chem Int Ed 44: 5115–5118
16. Kakiuchi K, Hosono E, Imai H, Kimura T, Fujihara S (2006) J Cryst Growth 293:541–545
17. Liu B, Aydill ES (2009) J Am Chem Soc 131:3985–3990
18. Ahmad MK, Murakami K (2011) Adv Mater Res 222:24–27
19. Ahmad MK, Murakami K (2012) Adv Res Phys 3(2):21208–21211
20. Mohan VM, Murakami K (2011) Adv Res Phys 2(2): 21112–21117